Preliminary communication / Communication

FTIR determination of adsorption characteristics for volatile organic compounds removal on diatomite mineral compared to commercial silica

Hicham Zaitan, Tarik Chafik *

Laboratoire de génie chimique et valorisation des ressources, faculté des sciences et techniques de Tanger, université Abdelmalek-Essadi, B.P. 416 Tangier, Morocco

Abstract

Gas phase FTIR measurement has being used to determine adsorbents characteristics such as adsorption capacity and isotherm. The experimental approach was applied to compare adsorption performances in terms of volatile solvent (*o*-xylene) adsorption and desorption for low cost diatomite mineral and commercial silica. The Langmuir equation was suggested to correlate the experimental isotherm. This assumption allowed an estimation of adsorbed molecular density within a monolayer, on the basis of the agreement obtained in *o*-xylene vapor pressure range where Langmuir model holds. ***To cite this article: H. Zaitan, T. Chafik, C. R. Chimie 8 (2005).***

Résumé

Une méthode expérimentale basée sur la mesure de spectres IRTF en phase gazeuse enregistrés dans des conditions dynamiques (sous flux de gaz à la pression atmosphérique) a été utilisée pour la détermination des capacités et des isothermes d'adsorption. L'approche a été appliquée pour comparer les performances d'un minerai diatomite avec celles d'une silice commerciale en terme d'adsorption et de désorption d'un composé organique volatil de type *o*-xylène. Une estimation de la monocouche de l'*o*-xylène adsorbée a été faite en se limitant au domaine de pressions où le modèle de Langmuir s'applique. ***Pour citer cet article : H. Zaitan, T. Chafik, C. R. Chimie 8 (2005).***

---

* Corresponding author.

E-mail address: chafik@fstt.ac.ma (T. Chafik).

1. Introduction

The treatment of volatile organic compounds' (VOCs) emissions in industrial plant is subject of great concern because of its harmful effect on human health and environment [1]. Removal technology based on adsorption is chosen mainly because of high elimination efficiency as well as economical advantages such as solvent recovery for reuse and low energy cost [2,3]. For such applications, activated carbon is widely used regarding its properties [4]. Nevertheless, such adsorbents become inappropriate if the adsorbed solvents to be recovered are flammable [5]. In this case materials like zeolites, alumina or polymers become of interest [6–9]. Hence continuous efforts are focusing on investigating adsorbent material that associate efficiency and low cost.

The present work aimed at investigating a local mineral, known as diatomaceous silica or kieselguhr, and valorizing it as a VOC adsorbent. This material gave promising results during its application for removing water pollutants such as atrazine, organophosphorus pesticides or silver [10,11]. In this study *o*-xylene was chosen as a representative of VOC, regarding its multiple uses in many chemical industries. The adsorption performances of the mineral were compared to those of silica, which was the main component of diatomite. The mineral presented an economic advantage in terms of a lower cost of 0.25 \$ kg^{-1} [12], as compared with a price of about 60 \$ kg^{-1} for silica aerosil.

The main objective of this work was to illustrate the suitability of an easy and efficient method for adsorption characteristics' investigations. The experimental approach is based on gas phase FTIR monitoring during dynamical adsorption and desorption. The obtained adsorption capacities yield to adsorption isotherm. The latter allowed, furthermore, an estimation of the adsorbed *o*-xylene monolayer in the range of *o*-xylene partial pressures where Langmuir equation holds.

2. Experimental

2.1. Experimental apparatus and methods

Dynamic adsorption/desorption experiment were carried out using a home-made device consisting of an assembly (Fig. 1) that permits (*i*) to prepare model gas mixture and flow rate control, (*ii*) to perform in situ pre-treatment, adsorption and desorption tests in quartz micro-reactor, (*iii*) to monitor *o*-xylene concentration in the gas flow at the reactor outlet using FTIR spectrometry or gas chromatography.

The experiments were carried out under dynamic conditions at atmospheric pressure, with respective masses of 1 and 0.1 g of diatomite and silica. Nitrogen was used as carrier gas to make *o*-xylene/N_2 mixture. The latter, was sent into the quartz reactor through six way valve V_{6H}. The concentration of *o*-xylene in the mixture was obtained using a saturator (S1) associated with a condenser (C1) immersed in a thermostatically controlled bath. This temperature was permanently checked so as to maintain constant *o*-xylene vapor pressure and consequently keep the *o*-xylene concentration unchanged. Attention was paid to hold always the *o*-xylene partial pressure lower than the vapor pressure value at adsorption temperature in order to avoid *o*-xylene condensation in gas phase. In addition, all tubes, valves and connections of the experimental apparatus were permanently heated.

Prior to each set of adsorption–desorption experiment, the solids were treated under air flow in the quartz micro-reactor. The treatment consists in gradually heating (5 K min^{-1}) until 473 K for diatomite and 573 K for silica, and maintaining the final temperature for 1 h before cooling to room temperature. Following this pretreatment, the adsorption step was carried out with a flow of 100 cm^3 min^{-1} of *o*-xylene/N_2 model mixture. Once the solid saturated, the gas mixture was shifted again to N_2 flow to proceed with isothermal desorption until the *o*-xylene response reached zero. Subsequent desorption under a progressive heating was necessary to achieve complete regeneration of the solids. During all these steps (1 cycle), the response of the system was monitored by measuring the gas mixture composition (X_{out} *o*-xylene molar fraction or partial pressure) at the reactor outlet. Note that *o*-xylene molar fraction X_{in} before contact gas/solid correspond to P/P_0, where P is vapor pressure of *o*-xylene and $P_0 = 760$ Torr. The *o*-xylene concentration in the gas stream at the reactor outlet was monitored with a FTIR Jasco 410 spectrometer (resolution of 4 cm^{-1}) using a Pyrex gas cell equipped with CaF_2 windows. This was achieved owing to multiples advantages offered by FTIR instrumentation such as rapid spectra acquisition and easy quantitative analysis, especially in case when they are no IR
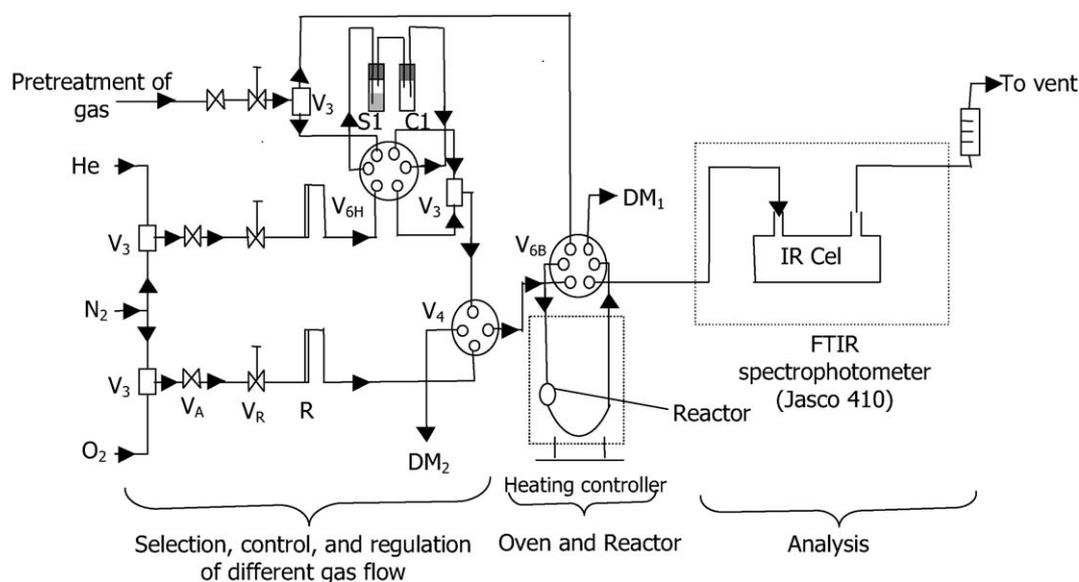
Fig. 1. Schematic flow sheet of the experimental apparatus used for *o*-xylene adsorption/desorption experiments.
VA, VR: Metering valves; V3: 3-way valve; V4: 4-way valves; V6: 6-way-valves; R: rotameter, DM_i : flowmeters; S and C: saturator and condenser.

bands overlapping [13,14]. Moreover, the use of FTIR was found to be very effective because it allowed, also, detection of further IR bands indicating the formation of new species in the gas stream (> 50 ppm) during the adsorption or desorption process. The molar fraction of *o*-xylene was given by the integration of its IR bands located between 2600 and 3200 cm^{-1} (Fig. 2) according to the Beer–Lambert law relating IR bands area to concentration [15–18]. Thus, preliminary calibration with *o*-xylene/N_2 mixtures of known composition was carried out using reactor by pass with V_{6B} 6-way valve, in order to correlate band area with concentration. Hence, the FTIR response to *o*-xylene contained in the

gas flow was found to produce linear plot in the studied concentration range and its accuracy was also verified with gas chromatography.

The evolution of the *o*-xylene concentration at the reactor outlet obtained from FTIR spectra during adsorption process permitted the monitoring of adsorbent loading as function of time (i.e. breakthrough curve). The numerical integration of the area below this curve yields to adsorption capacity considering the curve corresponding to the reactor response in the absence of solid (Figs. 3 and 4). This feature corresponds to the amount of adsorbed molecules expressed in µmol g^{-1} or µmol m^{-2}. The graphical representation
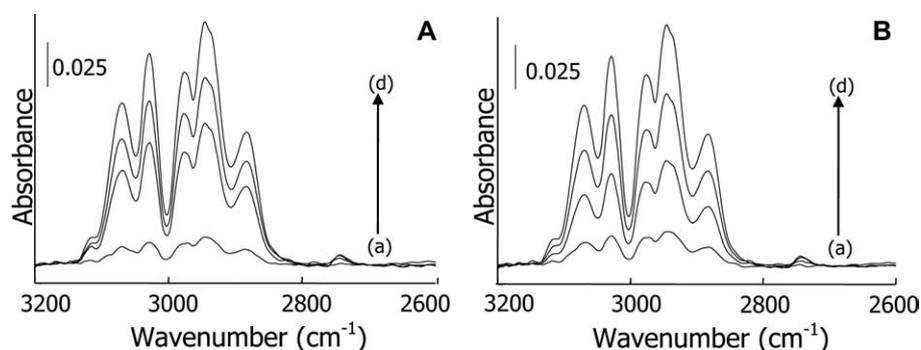
Fig. 2. Evolution of *o*-xylene IR bands during isothermal adsorption of 0.36% *o*-xylene/N_2 mixture at 300 K on diatomite (**A**) after (a)–(d) 6, 14, 18 and 38 min; and silica (**B**) after (a)–(d) 2, 10, 14 and 54 min.
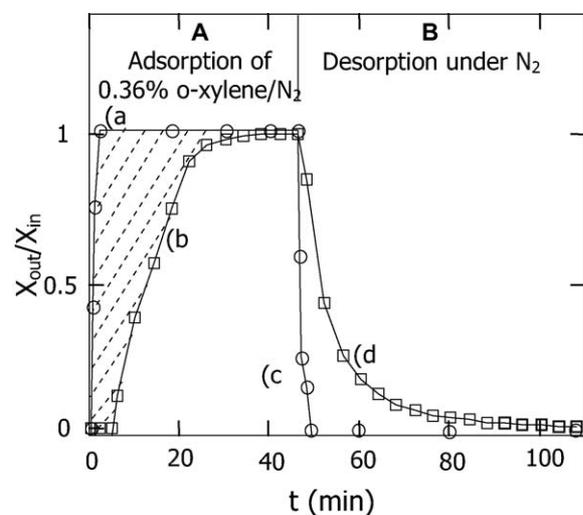
Fig. 3. *o*-Xylene concentration in the gas flow at the reactor outlet during adsorption of 0.36% *o*-xylene/N$_2$ at 300 K followed by isothermal desorption on 1 g of diatomite: (A) reactor response without solid under reaction mixture (B) breakthrough curve C) reactor by pass (D) desorption under N$_2$ at 300 K.
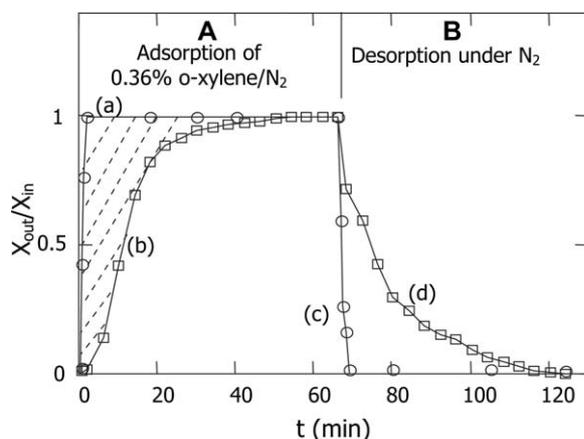
Fig. 4. *o*-Xylene concentration in the gas flow at the reactor outlet during adsorption of 0.36% *o*-xylene/N$_2$ at 300 K followed by isothermal desorption on 0.1 g of SiO$_2$ pretreated: (**A**) Reactor response without solid under reaction mixture (**B**) breakthrough curve (C) reactor by pass (D) desorption under N$_2$ at 300 K.

of the adsorption capacity versus *o*-xylene vapor partial pressure yields the adsorption isotherm. The same procedure was applied to obtain the amount of desorbed *o*-xylene.

2.2. Materials

The diatomite mineral tested in the present work comes from the deposits of Nador area in the north of Morocco. The mineral was found to be a mixture of Kaolinite, dolomite and halite with a major chemical composition of SiO$_2$. The adsorptive properties were compared to a commercial SiO$_2$ aerosil 200 m^2 g^{-1} provided by the Degussa Company. The chemical composition, BET surface and apparent density of the solids are given in Table 1.

3. Results and discussion

3.1. Breakthrough curves and adsorption capacity

The evolution of *o*-xylene IR bands during the course of isothermal adsorption at 300 K is given by Fig. 2A, B, respectively, for diatomite and silica. A gradual increase in intensity of *o*-xylene IR bands until adsorbent saturation is clearly evidenced. The concentration at the reactor outlet and inlet were then similar, meaning that equilibrium has been reached (spectra d of Fig. 2 after 38 and 54 min adsorption on diatomite and silica).

The aforementioned quantitative treatment procedure gives access to the breakthrough curves of Figs. 3A and 4A, where the evolution of *o*-xylene concentration in the gas flow was represented as relative values (X_{out}/X_{in}). The adsorbed amounts were obtained by the integration of the area between the curves a and b (dashed area of Figs. 3A and 4A) corresponding to the

Table 1
Chemical composition (weight %) and BET surface of diatomite and SiO$_2$

Solids	SiO$_2$	Al$_2$O$_3$	Fe$_2$O$_3$	Na$_2$O	K$_2$O	MgO	TiO$_2$	CaO	Surface area (m^2 g^{-1})	Apparent density (g l^{-1})
Diatomite	72.8	5.22	1.94	0.83	0.901	1.13	0.27	5.86	21	326
SiO$_2$	99.9	< 500 (ppm)	< 30 (ppm)	–	–	–	< 300 (ppm)	–	200	50

reactor responses in the absence and presence of solids, according to Eq. (1):

$$QT_{o\text{-xylene}} = \frac{F \times X_{in}}{W} \left[t_s - \int_0^{t_s} \frac{X_{out}}{X_{in}} \, dt \right] \qquad (1)$$

where $QT_{o\text{-xylene}}$ is the adsorbed amount of o-xylene at saturation (adsorption capacity), X_{in}, X_{out} the molar fractions of o-xylene at reactor inlet and outlet, W the mass of absorber, t_s the saturation time and F the gas molar flow rate. It should be stated that the adsorption process occurred in a micro-reactor under isothermal conditions in which the pressure drop as well as the variation in fluid velocity between the reactor inlet and outlet were considered negligible. Hence, the integration of the breakthrough curves according to Eq. (1) for a 0.36% o-xylene in N_2 yields values of 197 and 1958 μmol g^{-1}, respectively, for diatomite and SiO_2.

Therefore, as reported by Ruthven [7], such a method is valid only if the gas speed is constant along the reactor bed. Thus, it is appropriate to point out that in case of a non-negligible difference between the overall flows at the reactor inlet and outlet, the absolute amount of adsorbed o-xylene could be obtained from Eq. (2). Accordingly, the results given by Eq. (1) were correct because the o-xylene was highly diluted in nitrogen ($X_{out} < X_{in} \ll 1$).

$$QT_{o\text{-xylene}} = \int_0^{t_s} \frac{F_{in}}{W} \cdot \frac{(X_{in} - X_{out})}{(1 - X_{out})} \, dt \qquad (2)$$

3.2. o-Xylene desorption and solids regeneration

Following solids' saturation with adsorbed o-xylene, the gas mixture was changed to N_2 flow in order to perform isothermal desorption. The evolution of o-xylene IR bands recorded during this step showed a gradual decrease of o-xylene IR bands intensity with time on stream (spectra not shown). The application of the previous treatment to the recorded spectra permitted a quantification of the reversibly adsorbed o-xylene (curves (d) in Figs. 3B and 4B). It was found that after ~60 min on N_2 stream at 300 K, 137 and 1635 μmol g^{-1} of o-xylene desorbed, respectively, from diatomite and SiO_2. Although the o-xylene response reached zero, the desorbed amounts represented only 70% and 80% from the total adsorbed o-xylene. Complete desorption,

required subsequent heating (5 K min^{-1}) up to 473 and 573 K, respectively, for diatomite and silica. On the other hand, the FTIR spectra recorded during heating under N_2 flow do not exhibit any new species formation (spectra not shown). This indicates that both solids do not have any catalytic activity that may lead to o-xylene decomposition. The repetition of the adsorption regeneration cycles for more than three times led to a modification of silica color (dyed brown) associated with a reduction in its adsorption capacity. A treatment at 710 K under air flow permitted to restore the initial performances of the silica. So far, the mineral was hardly affected by this desactivation and a thermal treatment up to 473 K was enough to recover the initial performances. This is considered to be an additional advantage of diatomite mineral with respect to easier regeneration.

3.3. Adsorption isotherm and monolayer

The same approach based on dynamical adsorption was used for the determination of adsorption isotherms. The investigations were carried out at 300 K using different concentrations of o-xylene in the gas flow. As stated above, to avoid any condensation of o-xylene in the gas phase, the adsorption experiments were performed with reaction mixtures in which the partial pressure of o-xylene (P) was kept lower than the o-xylene vapor pressure (P_s) at the adsorption temperature ($P < P_s = 6.62$ torr at 300 K calculated from Antoine equation). This technically allowed us to work with a limited o-xylene pressures ranging from 0.7 to 5.8 torr. The adsorbed amounts corresponding to saturation were obtained by integration of the breakthrough curves presented in Figs. 5 and 6 (results summarized in Table 2). These data lead to the adsorption isotherms of Fig. 7, giving the evolution of saturation adsorbed amounts versus o-xylene pressure. The increase shown for the uptaked amounts with the o-xylene pressure augmentation was also reported in the literature for VOC adsorption studies under dynamic conditions [19,20].

Langumir equation, considered as the simplest and most useful model for adsorption phenomenon, has being used to correlate our experimental data and hence estimate the monolayer density.
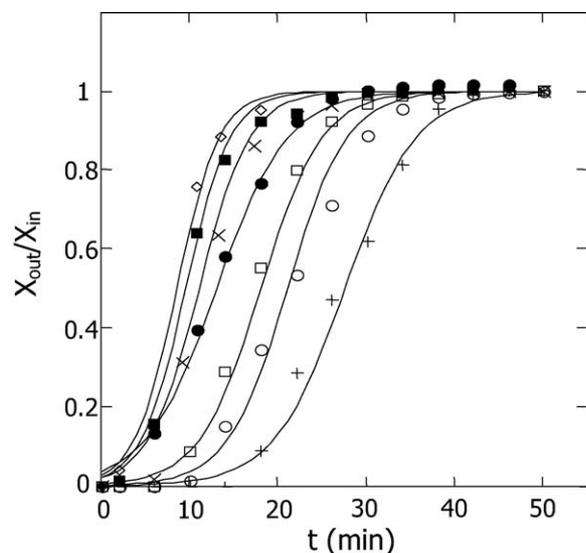
Fig. 5. Breakthrough curves obtained with 1 g of diatomite at 300 K for different *o*-xylene vapor pressure: ◇, P*o*-xylene=5.86; ■, 4.88; ×, 3.49; ●, 2.7; □, 1.802; ○, 1.25; and +, 1.06 Torr.

Fig. 6. Breakthrough curves at 300 K obtained with 0.1 g of SiO₂: for different *o*-xylene vapor pressure: ◇, P*o*-xylene= 5.86; ■, 4.88; ×, 3.49; ●, 2.7; □, 1.802; ○, 1.25; and +, 0.7 Torr.

According to Langumir:

$$\theta = \frac{K\,P}{1 + K\,P}, \text{ with } \theta = \frac{N}{N_m}$$

(*N*: mole number of adsorbed *o*-xylene and N_m: mole number adsorbed within monolayer). $K = \frac{k_a}{k_d}$: adsorption/desorption coefficient and *P* the *o*-xylene pressure.

The linearity obtained from the plot of $1/N$ versus $1/P$, shown in Fig. 8, confirms the agreement between Langmuir equation and our experimental data in the studied *o*-xylene pressure range. It should be stated, however, that this model may not be valid if we pro-

ceed with adsorption pressures up to much higher values. Nevertheless, the straight line obtained in the range where Langumir equation holds intercepts at $1/N_m$ and enables us to estimate a mole number of *o*-xylene adsorbed within monolayer. Therefore, values of 420 and 4000 μmol g⁻¹ were obtained for N_m, respectively, for diatomite and silica. Considering the surface area, an approximate density of ≈20 μmol m⁻² for the two solids (S_{BET} Diatomite = 21 m² g⁻¹ and S_{BET} silica = 200 m² g⁻¹). These results were compared to some data given in the literature for xylene adsorption on zeolite type at 298 K [21,22] and activated carbon [23]. The reported values of adsorption capacities of xylene isomers on NaY, KY and BaY zeolites, were respectively 2164, 2011, 1801 μmol g⁻¹ for *p*-xylene

Table 2

Amounts of adsorbed *o*-xylene (in μmol g⁻¹) obtained from breakthrough curves of Figs. 5 and 6

o-Xylene vapor pressure (Torr)	Concentration of *o*-xylene in the gas stream (%)	Diatomite Adsorbed total quantity (μmol g⁻¹) at 300 K	SiO₂ Adsorbed total quantity (μmol g⁻¹) at 300 K
0.7	0.1	–	700
1.06	0.14	108	–
1.25	0.164	123	1134
1.8	0.237	155	1425
2.72	0.36	197	1958
3.5	0.46	223	2100
4.88	0.64	255	2400
5.86	0.77	275	2590
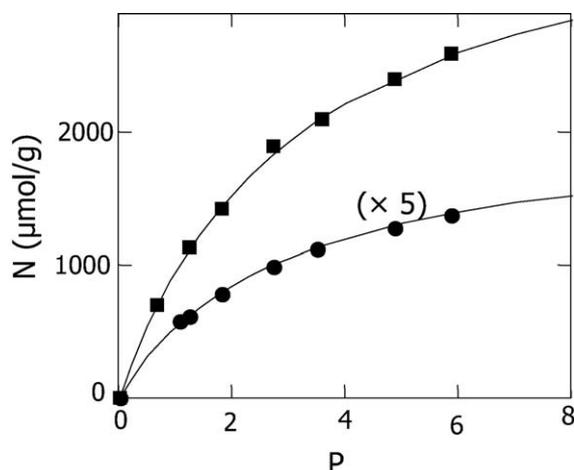
Fig. 7. Adsorption isotherm of *o*-xylene at 300 K on diatomite (●) and SiO₂ (■).
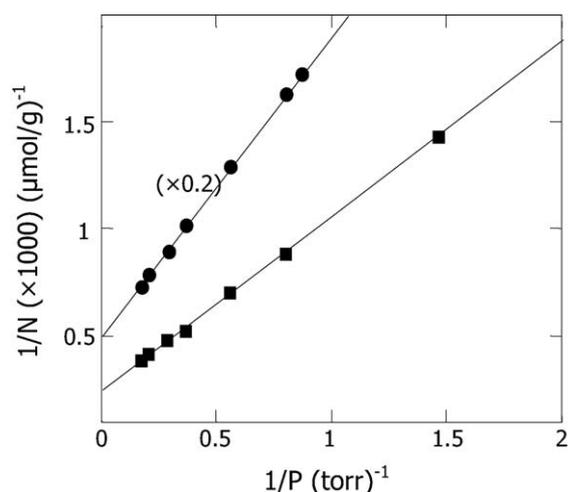
Fig. 8. Langmuir equation $1/N = f(1/P)$ for *o*-xylene adsorption at 300 K on diatomite (●) and on silica (■).

and 2258, 1982, 1778 μmol g^{-1} for *m*-xylene. Due to its higher BET surface (1330 m^2 g^{-1}), the activated carbon AC40 presented the highest adsorption capacity of 6290 μmol g^{-1} [23]. However, the expression of the latter value in μmol m^{-2} yields to ~5 μmol m^{-2}, which is lower, as compared with the monolayer density obtained with diatomite and silica (~20 μmol m^{-2}).

4. Conclusion

The main objective of our work was to illustrate the interest of an easy and efficient method for the evaluation of adsorption characteristics. The experimental approach was based on FTIR spectra measurements during adsorption and desorption under gas flow at atmospheric pressure. The technique permitted determination of adsorption capacity, adsorption isotherm as well as determination of reversible and irreversible amounts. Additional information was supplied by detection of further decomposition and/or reaction of adsorbed molecule.

The procedure has being applied to compare adsorption performances of low-cost local mineral with those of commercial silica with respect to *o*-xylene adsorption and desorption. The obtained results showed that the loading capacity of commercial silica was higher than diatomite mineral, due to its greater BET surface. However, the mineral was found to be more easily regenerated and could be of interest, particularly, for high-cost solvent recovery. Furthermore, the experimental adsorption isotherm allowed also an estimation of the adsorbed molecular density within a monolayer. This finding was supported by the agreement between our results and the Langmuir model in the studied *o*-xylene partial-pressure range.

References

[1] N. Godinot, G. Sicard, D. Dubois, Odours VOC's J. 1 (1995) 202.
[2] J.S. Waston, Separation Methods for Waste and Environmental Applications, in: Marcel Dekker, New York, 1999, pp. 23–32.
[3] M.J. Ruhl, Chem. Eng. Prog. 89 (1993) 37.
[4] M. Suzuki, Carbon 32 (1994) 577.
[5] S.W. Blocki, Environ. Prog. 12 (1993) 226.
[6] Y. Takeuchi, I. Hayato, N. Miyata, S. Asano, Sep. Technol. 5 (1995) 23.
[7] D.M. Ruthven, Principles of Adsorption Processes, Wiley, New York, 1984.
[8] P. Gélin, J.F. Dutel, B.F. Mentzen, Micropor. Mater. 4 (1995) 283.

[9] K. Carsten, W. Meininghaus, R. Prins, Micropor. Mesopor. Mater. 35 (2000) 349.

[10] A. Ridha, H. Aderdour, H. Zineddine, M.Z. Benabdallah, M. El Morabit, A. Nadiri, Ann. Chim. Sci. Matér. 23 (1998) 161.

[11] K. Agdi, A. Bouaid, A. Martin Esteban, P. Fernandez Hernando, A. Azmani, C. Camara, J. Environ. Monit. 2 (2000) 420.

[12] US Geological Survey Mineral Commodity Summaries, January 2004.

[13] D. Bianchi, J.L. Gass, C. Bouly, D. Maret, SAE paper 910839 (1992).

[14] D.J. Kim, J.M. Kim, J.E. Yie, S.G. Seo, S.C. Kim, J. Colloid Interface Sci. 274 (2) (2004) 538.

[15] P.B. Rasband, W.C. Hecker, J. Catal. 139 (1993) 551.

[16] S. Zeradine, A. Bourane, D. Bianchi, J. Phys. Chem. B 105 (2001) 7254.

[17] T. Chafik, O. Dulaurent, J.L. Gass, D. Bianchi, J. Catal. 179 (1998) 503.

[18] X. Mugniery, T. Chafik, M. Primet, D. Bianchi, Catal. Today 52 (1999) 15.

[19] Z.-H. Huang, F. Kang, Y.-P. Zheng, J.-B. Yang, K.-M. Liang, Carbon 40 (2002) 1363.

[20] J. Benkhedda, J.N. Jaubert, D. Barth, C. Zetzl, G. Brunner, Sep. Sci. Technol. 36 (10) (2001) 2197.

[21] M.H. Simonot-Grange, O. Bertrand, E. Pilverdier, J.P. Bellat, C. Paulin, J. Therm. Anal. 48 (1997) 741.

[22] E. Pilverdier, Thesis, University of Bourgogne, Dijon, France, 1995.

[23] J. Benkhedda, J.N. Jaubert, D. Barth, L. Perrin, M. Bailly, J. Chem. Thermodyn. 32 (3) (2000) 411.